7-25-1988

GaAs/GaAlAs distributed Bragg reflector laser with a focused ion beam, low dose dopant implanted grating

M. C. Wu

M. M. Boenke

S. Wang

W. M. Clark Jr.

E. H. Stevens

See next page for additional authors

GaAs/GaAlAs distributed Bragg reflector laser with a focused ion beam, low dose dopant implanted grating

M. C. Wu, M. M. Boenke, and S. Wang
Department of Electrical Engineering and Computer Sciences, Electronics Research Laboratory, University of California, Berkeley, California 94720

W. M. Clark, Jr., E. H. Stevens, and M. W. Utiaut
Hughes Research Laboratories, Malibu, California 90265

(Received 18 March 1988; accepted for publication 31 May 1988)

We report, for the first time, the performance of a GaAs/GaAlAs distributed Bragg reflector (DBR) laser using a focused ion beam implanted grating (FIB-DBR). Stripes of Si^{++} with a period of 2300 Å and a dose $\sim 10^{14}$ cm^{-2} are directly implanted into the passive large optical cavity layer to provide the distributed feedback. Surface-emitting light from the second-order grating is observed. Threshold current of 110 mA and single DBR mode operation from 20 to 40 °C are obtained. The wavelength tuning rate with temperature is 0.8 Å/°C. The coupling coefficient is estimated to be 15 cm^{-1}. The results show that FIB technology is practical for distributed feedback and DBR lasers and optoelectronic integrated circuits.

Distributed feedback (DFB) lasers[1] and distributed Bragg reflector (DBR) lasers[2–5] are the most important single-wavelength light source for optical communications and optoelectronic integrated circuits. Conventional gratings providing the distributed feedback are usually fabricated with holographic lithography and etching.[1-5] With this technique it is difficult to fabricate lower order gratings, which have the benefits of larger coupling efficiency and lower radiation loss. A large coupling constant, κ, is important for stable single-mode operation under high-frequency modulation[6] and for wider wavelength tuning range in DBR lasers.[7] Electron beam lithography[8] has the capability of writing first-order gratings; however, this requires the use of very thin layers of photoresist ($\approx$200 Å) for which proper step coverage is often a problem.

Use of focused ion beam (FIB) implantation offers significant advantages to the fabrication of these gratings because the technique is freed from the resolution and alignment difficulties associated with resist-mask-dependent processing. With FIB it is possible to vary the dose, stripe width and spacing, and ion and implant energy with great flexibility to make the grating structure. These advantages have been demonstrated previously in semiconductor electronic device fabrication including metal-semiconductor field-effect transistors (MESFET's) with a striped channel structure[9] and laterally profiled active area implants to reduce the Kirk effect in bipolar transistors.[10] In semiconductor lasers FIB micromachining has been utilized to provide facet etching and coupled-cavity lasers.[11] The FIB implant and prolonged high-temperature annealing was used to produce disordering in superlattices.[12] These uses of the FIB require either implant doses much higher than 10^{15} cm^{-2}, which necessitate very long FIB processing times, or long annealing time, which precludes the fabrication of fine features, and do not emphasize the flexible advantages of the tool. Our theoretical calculations show that grating coupling strengths on the order of 10–100 cm^{-1} that are suitable for DFB and DBR lasers would be possible using dopant implants more than ten times less.[13]

Operation of FIB-implanted grating is based on the free-carrier-induced index change. Free carriers in semiconductors will reduce the refractive index n through carrier-induced shift of absorption edge ($\partial n/\partial N \sim 10^{-20}$ cm^3)[14] and free-carrier-plasma effect ($\partial n/\partial N \sim 10^{-21}$ cm^3). Such index change ($\Delta n \sim 0.05$) is somewhat smaller than that produced by a conventional composition-varied grating ($\Delta n \sim 0.2$). Therefore, the laser cavity must be designed to maximize the effect. In this letter, we report the performance of a DBR laser with a second-order FIB-implanted grating.

The schematic of the laser structure is shown in Fig. 1. A coupled active-passive large optical cavity (LOC) structure is used. The layers above the LOC are removed in the passive section, and the grating is formed by direct FIB implantation into the LOC layer to maximize the overlap of the field and the grating. The fabrication process is described in the following. First, five layers are grown successively by liquid phase epitaxy: 1.5-μm-thick n-$Ga_{0.7}Al_{0.3}As$ cladding layer, 0.5-μm-thick n-$Ga_{0.85}Al_{0.15}As$ LOC layer, 0.1-μm-thick undoped GaAs active layer, 1.3-μm-thick p-$Ga_{0.7}Al_{0.3}As$ upper cladding layer, and finally 0.3-μm-thick p^+-GaAs cap layer. After growth, the active part is masked by Si_3N_4 and the upper cladding layer in the passive section is selectively removed by KI-I_2 (113 g KI, 65 g I_2, and 100 cc H_2O). The exposed active layer is then etched away by 1:1:20 ratio of NH_4OH:H_2O_2:H_2O. A ridge waveguide of width 10 μm is formed in the active area along the [011] direction, and a 16-μm-wide shallow ridge waveguide is also formed in the passive LOC section to improve lateral guiding and matching with the active guide.

The gratings were produced via FIB implants of Si. Silicon was chosen because (1) the free-carrier-induced index change is larger for n-type dopants[14] and (2) the low diffusivity of Si ensures minimal spreading of the grating pattern during annealing. The Si stripes were produced by scanning the FIB from a three-lens, mass-separating, variable-energy ion focusing column.[15] Dose was varied from 4 to 8×10^{14} cm^{-2} by changing the number of repetitive scans by the beam over the stripe. In calculating the number of scans

 0003-6951/88/300265-03$01.00

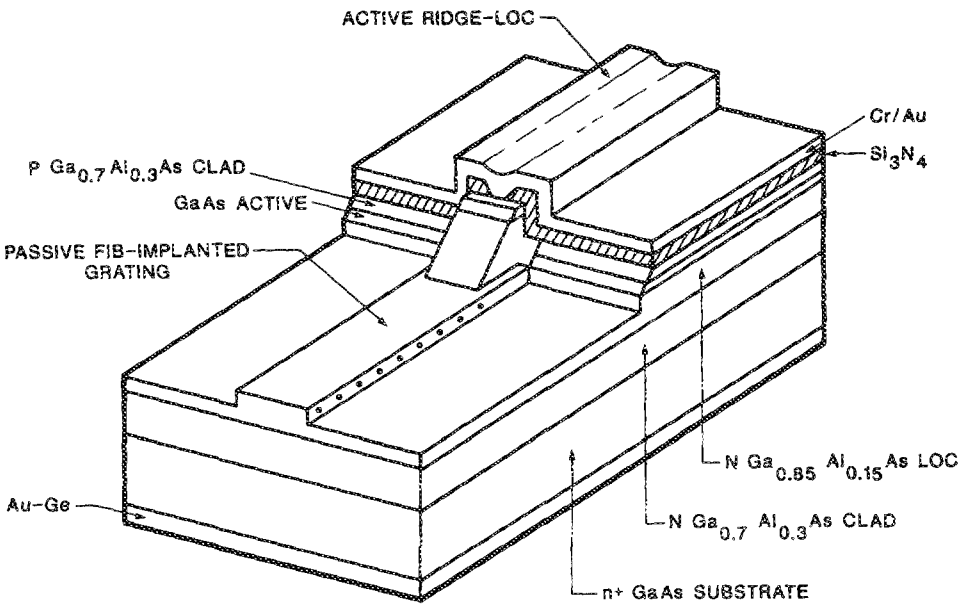

FIG. 1. Schematic drawing of the active-passive LOC DBR laser with FIB-implanted grating.

required for a given stripe dose, the stripe width was assumed to be that of the beam, that is, a full width at half maximum intensity (FWHM) of approximately 700 Å for a Gaussian current density profile. System accuracy for beam placement is estimated to be within 450 Å. The gratings were implanted at 100 keV and the second-order period was approximately 2300 Å. The wafer is then capped with thermal chemical vapor deposited (CVD) Si_3N_4 and rapid thermal annealed at 950 °C for 10 s. The encapsulation of the Si_3N_4 is very important to reduce the diffusivity of Si atoms in GaAs,[15] and negligible diffusion is obtained in this case.

After metallization and lapping, the laser is cleaved and mounted p-side up for measurement. There is no coating on either facet. First, the laser is inspected from the top surface to observe the surface-emitted light from the second-order grating. Figure 2 shows the near-field distribution along a laser with a long grating section ($L_G = 320\,\mu$m) and a short active section ($L_A = 160\,\mu$m). The cross-sectional schematic of the laser is shown in Fig. 2(a). Figure 2(b) shows the picture of the near field in which the white bar in the middle corresponds to the surface-emitted light deflected by the second-order grating. The circular spot at the left end of the white bar is due to imperfect matching of the waveguides at the transition region. From the line-scanned profile of the near field [Fig. 2(c)], the value of κ is estimated[17] to be 15 cm^{-1}.

The DBR mode is observed when the lasing wavelength is close to the Bragg wavelength λ_B ($\approx$8530 Å). Figure 3 shows the spectrum at various temperatures for a laser with $L_A = 290\,\mu$m, $L_G = 335\,\mu$m, and biased at 220 mA. The measurement is done under pulsed operation with a pulse width of 1 μs and repetition rate of 1 kHz. At 16.8 °C, the DBR mode at 8528 Å is far away from the gain peak at 8485 Å and the lasing is dominated by Fabry–Perot (FP) modes. The FP mode spacing of 3.1 Å indicates the lasing is between the cleaved front facet and the etched facet at the transition. As temperature increases, the gain peak shifts towards λ_B and the DBR mode gradually dominates and suppresses the FP modes. The gain peak coincides with λ_B at about 35 °C, at which strongest light intensity is observed. At higher temperature, side mode suppression becomes worse because of the increase in threshold current.

The variation of threshold current and lasing wavelength versus current is summarized in Fig. 4. The laser lases in single wavelength from 20 to 40 °C. The wavelength tuning rate of 0.8 Å/°C indicates that it is DBR mode. The threshold current variation with temperature follows a straight line with a characteristic temperature $T_0 = 110$ K except for a dip around 35 °C. The dip corresponds to the coincidence of the gain peak and λ_B. At room temperature, the threshold current is 110 mA.

Theoretically, the implanted grating can be approxi-

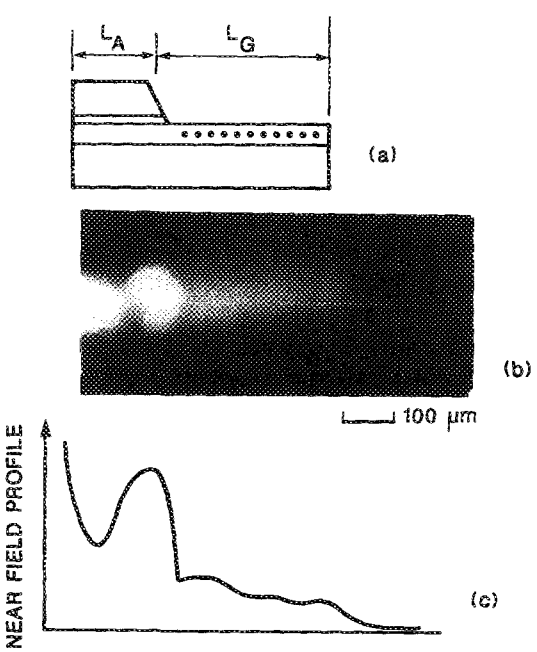

FIG. 2. (a) Schematic cross section of the DBR laser, (b) near-field picture of the surface-emitting light from the second-order FIB-implanted grating, and (c) the line-scanned profile of the near field.

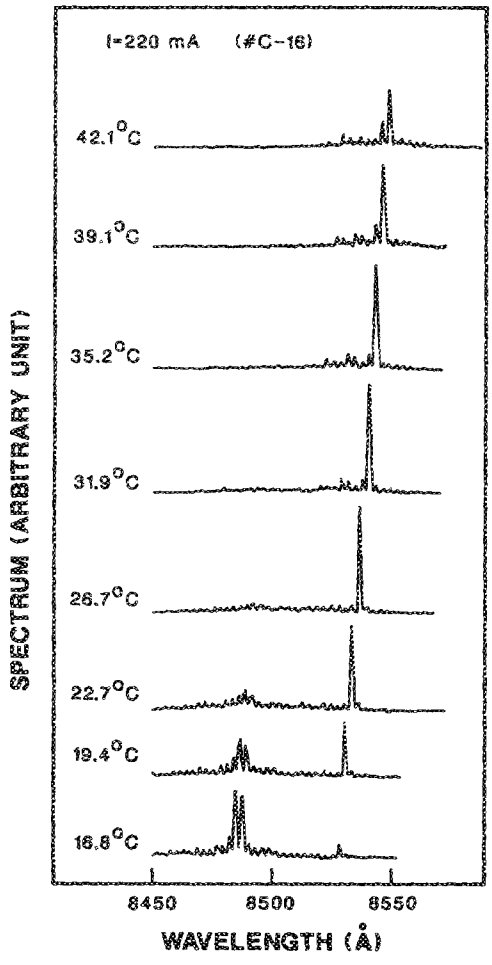

FIG. 3. Spectrum of the DBR laser at various temperatures. At low temperature (16.8 °C), FP modes (8480–8490 Å) of the active cavity dominate. As temperature increases, the gain peak shift toward Bragg wavelength ($\approx$8530 Å) and DBR mode emerge and suppress the FP modes.

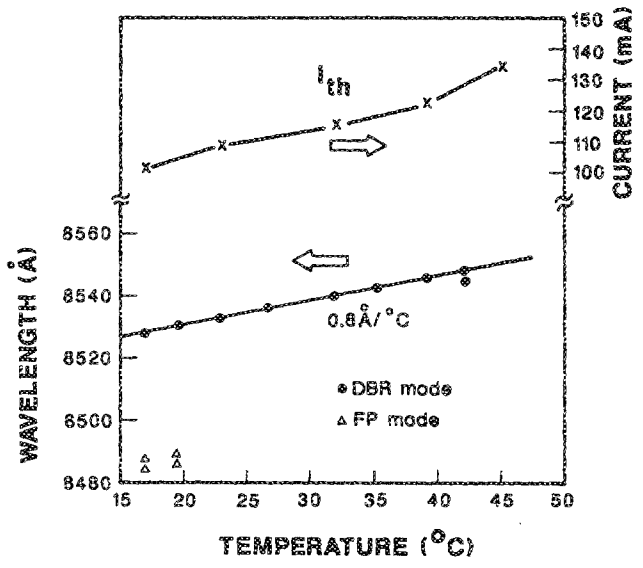

FIG. 4. Variation of threshold current I_{th} and lasing wavelength with temperature. The I_{th} followed a straight line except for a dip at around 35 °C, corresponding to the coincidence of the gain peak and the Bragg wavelength. Single wavelength operation is observed from 20 to 40 °C.

mated by an array of two-dimensional Gaussian functions of vertical straggle ΔR_p, horizontal straggle ΔR_t, period Λ, and centered at R_p below the surface. The activated electrons at the peak ($\approx 3\times 10^{18}$ cm^{-3} for our dose and annealing condition) decrease the refractive index by $\Delta n = 3\times 10^{-2}$. The corresponding change in effective refractive index $\Delta n_{\rm eff} = 0.004$ for $R_p = 0.10$ μm and $\Delta R_p = 0.045$ μm. The second-harmonic component of this index perturbation is $\Delta n_{\rm eff}^{(2)} = (\sqrt{2\pi}\Delta n_{\rm eff}\Delta R_t/\Lambda)e^{-(8\pi^2\Delta R_t^2/\Lambda^2)}$. For $\Delta R_t = 350$ Å, $\kappa = 2\pi|\Delta n_{\rm eff}^{(2)}|/\lambda_B = 18$ cm^{-1}, in good agreement with the experiment data. More complete theoretical calculation will be published elsewhere.[13] Though κ is not very large at present, it can be improved by a factor of 5 by reducing the thickness of the LOC layer, which effectively increases the overlap of light and grating. Reduction of the FIB linewidth would permit implanting a first-order grating, with which another factor of two increase in κ is expected.

In conclusion, we have demonstrated, for the first time, a GaAs/GaAlAs active-passive DBR laser with a FIB-implanted second-order grating. The laser has a threshold current of 110 mA and operates in a single DBR mode from 20 to 40 °C with a 0.8 Å/°C tuning rate. The coupling constant is estimated to be 15 cm^{-1}. An improvement in κ by an order of magnitude is achievable by reducing the thickness of the passive waveguide and with a first-order FIB-implanted grating. This technology is compatible with molecular beam epitaxy (MBE) and the FIB implant can be done *in situ* inside the MBE chamber. The experimental results show that the FIB is a promising technology for future DFB and DBR lasers and optoelectronic integrated circuits. This work was supported by Eastman Kodak, Bell Communications Research, and National Aeronautics and Space Administration grant No. NAG-1-580.

[1]Y. Nakano and K. Tada, Appl. Phys. Lett. **49**, 1145 (1986).
[2]F. K. Reinhart, R. A. Logan, and C. V. Shank, Appl. Phys. Lett. **27**, 45 (1975).
[3]W. T. Tsang and S. Wang, Appl. Phys. Lett. **28**, 596 (1976).
[4]G. A. Evans, J. M. Hammer, N. W. Carlson, F. R. Elia, E. A. James, and J. B. Kirk, Appl. Phys. Lett. **49**, 315 (1986).
[5]K. Kojima, S. Noda, K. Mitsunaga, K. Kyuma, and K. Hamanaka, Appl. Phys. Lett. **50**, 1705 (1987).
[6]J. Glinski and T. Makino, IEEE J. Quantum Electron. **QE-23**, 849 (1987).
[7]M. C. Wu, M. M. Boenke, M. Werner, F. Schiffmann, Y. H. Lo, and S. Wang, J. Appl. Phys. **63**, 291 (1988).
[8]A. S. Gozdz, P. S. D. Lin, A. Scherer, and S. F. Lee, Electron. Lett. **24**, 123 (1988).
[9]D. B. Rensch, D. S. Matthews, M. W. Utlaut, M. D. Courtney, and W. M. Clark, Jr., IEEE Trans. Electron Devices **ED-34**, 2232 (1987).
[10]R. H. Reuss, D. Morgan, A. Goldenetz, W. M. Clark, D. B. Rensch, and M. Utlaut, J. Vac. Sci. Technol. B **4**, 290 (1986).
[11]L. R. Harriott, R. E. Scotti, K. D. Cummings, and A. F. Ambrose, J. Vac. Sci. Technol. B **5**, 207 (1987).
[12]K. Ishida, K. Matsui, T. Funkunaga, J. Kobayashi, T. Morita, E. Miyauchi, and H. Nakashima, Appl. Phys. Lett. **51**, 109 (1987).
[13]M. M. Boenke, M. C. Wu, S. Wang, W. M. Clark, Jr., E. H. Stevens, and M. W. Utlaut (unpublished).
[14]D. D. Sell, H. C. Casey, Jr., and K. W. Wecht, J. Appl. Phys. **45**, 2650 (1974).
[15]V. Wang, J. W. Ward, and R. L. Seliger, J. Vac. Sci. Technol. **19**, 119 (1981).
[16]M. E. Greiner and J. F. Gibbons, J. Appl. Phys. **57**, 5181 (1985).
[17]S. Wang, in *Semiconductors and Semimetals*, edited by W. T. Tsang (Academic, New York, 1985), Vol 22, part E, p. 61.